Magnetar-like outburst from high-magnetic field radio/gamma-ray pulsar PSR J1119-6127

reporter : Huihui Wang
Supervisor:Jumpei Takata
wanghh@hust.edu.cn
Huazhong University of Science and Technology（HUST）

collaborators：
L.C.C. Lin, Jumpei Takata ,Kwan-Lok Li, Chin-Ping Hu, C. Y. Hui, Pak-Hin T. Tam, and C.-Y. Ng

outline

- introduction
- Gamma-ray / x-ray analysis
- conclusion

PSR J1119-6127

- The spin period : $P = 0.407s$
  - Spin down rate : $\dot{P} = 4.0 \times 10^{-12}$
- The characteristic age: $\tau < 2 \quad kyr$
- The magnetic field : $B = 4.1 \times 10^{13} G$
- Associated SNR : $G292.2 - 0.5$
- spin-down power: $\dot{E} = 2.3 \times 10^{36}$ ergs s^{-1}

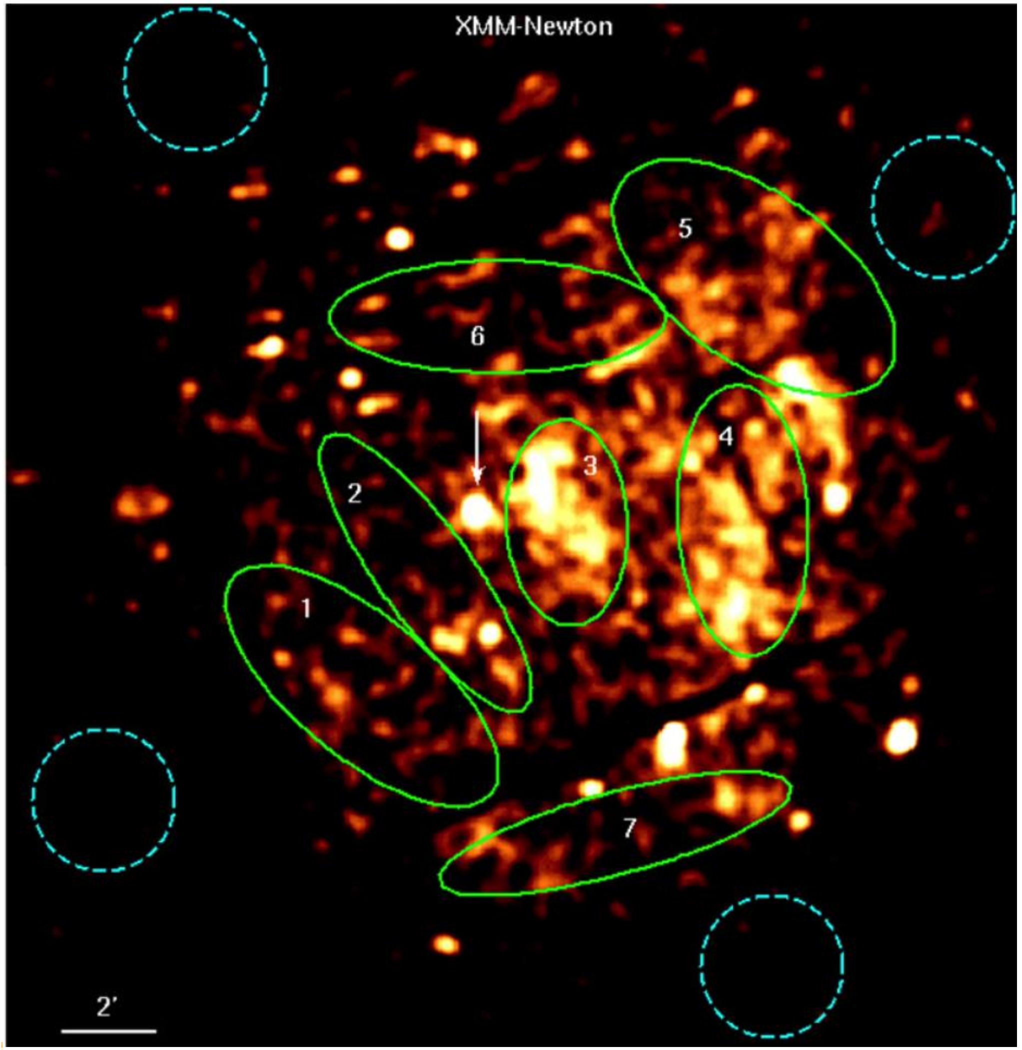

s

Strong magnetic field RPPs on P-Ṗ diagram

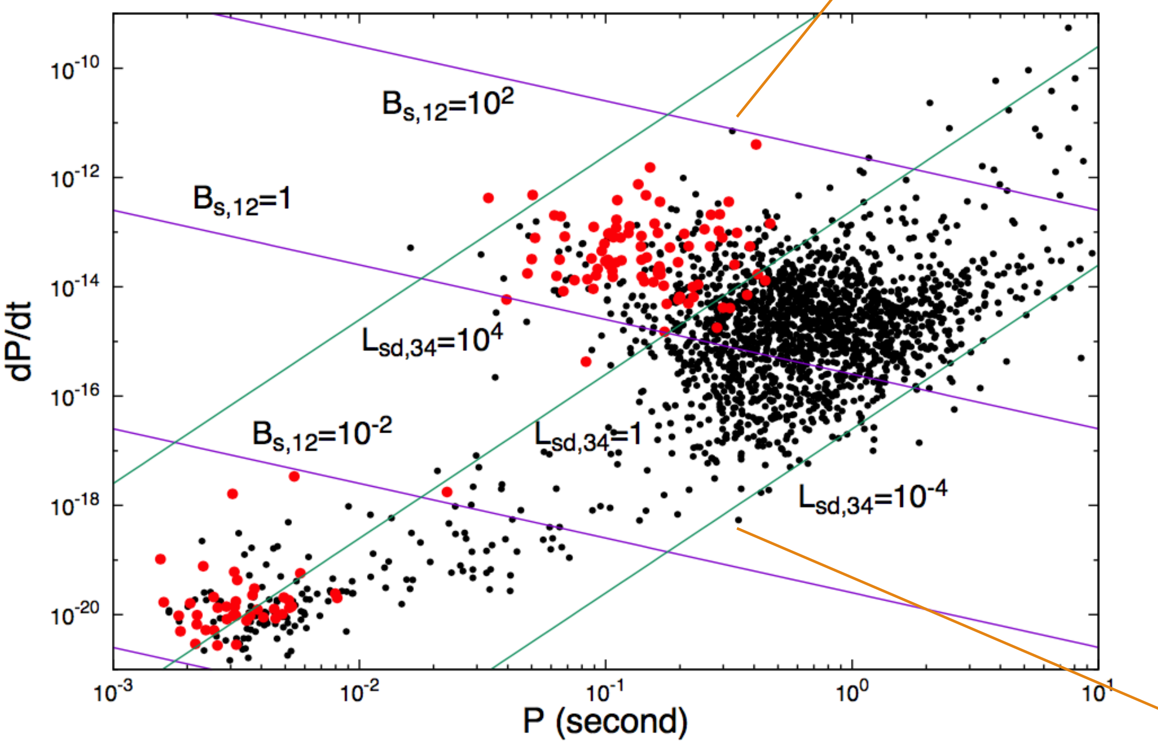

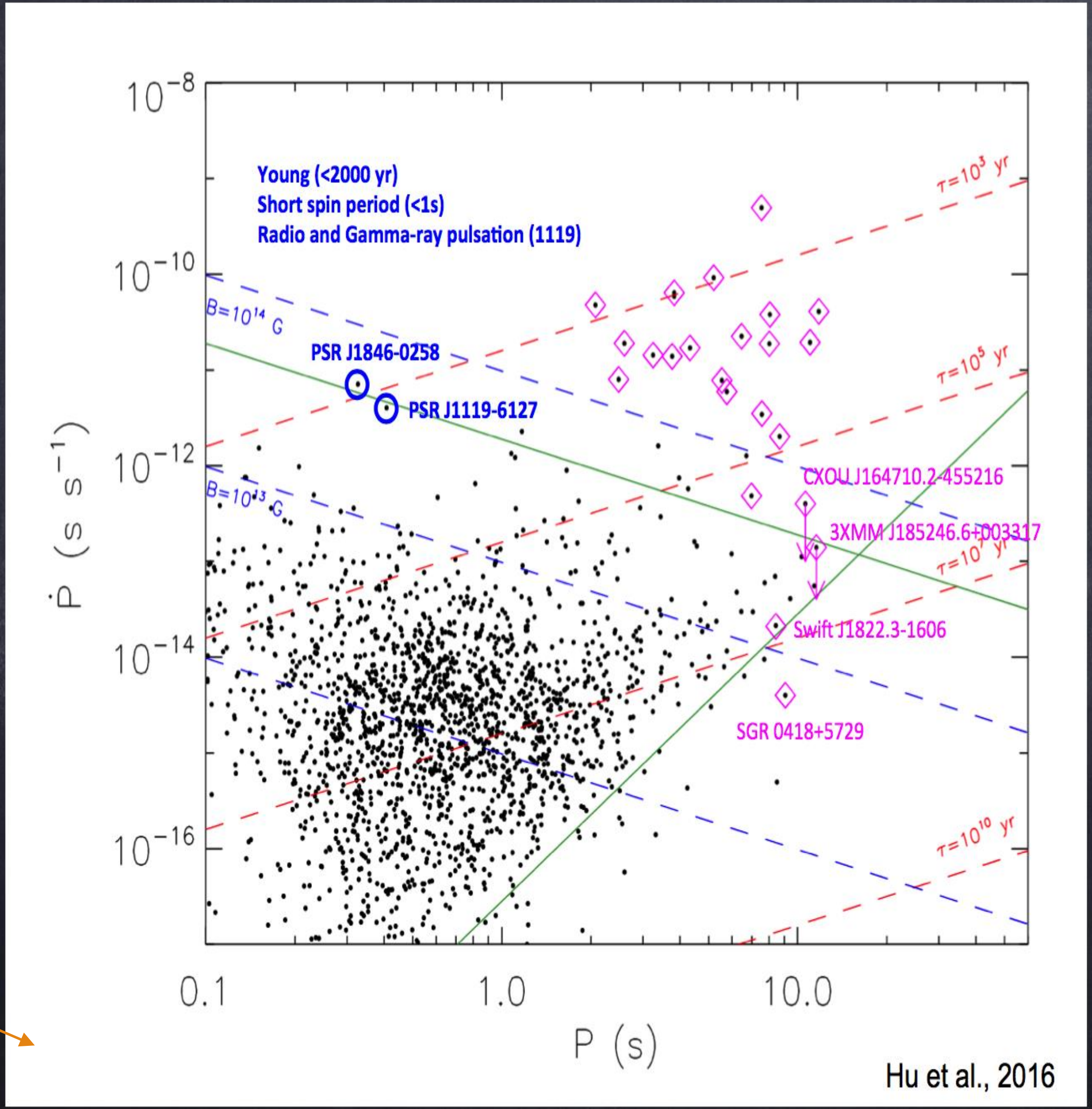

HUST

High-Magnetic field Pulsar

- **The magnetic field of PSR J1119-6127 ：** $B = 4.1 \times 10^{13} G$ ， it is around critical field of QED .(4.4X10^13 G)

  --One order of magnitude stronger than usual pulsars
  --One or two order of magnitude lower than magnetars.

- **Pulsed emission :** radio, X-ray and gamma-ray (typical young pulsar)

- **Glitch** : glitch in 2004 and large glitch in 2007,2016 (typical young pulsar)

2016 X-ray outburst

- Fermi/GBM triggered on a burst on 2016 July 27 (trigger: bn160727543) located within the error box of PSR J1119−6127，covering a duration of 0.040s 。

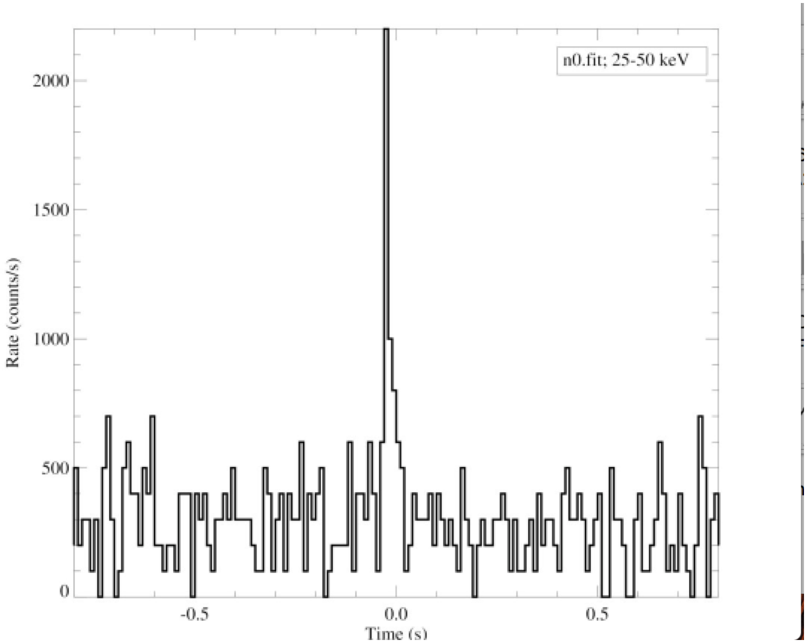

- Glitch with a size $\Delta\Omega/\Omega \sim 6 \times 10^{-6}$.

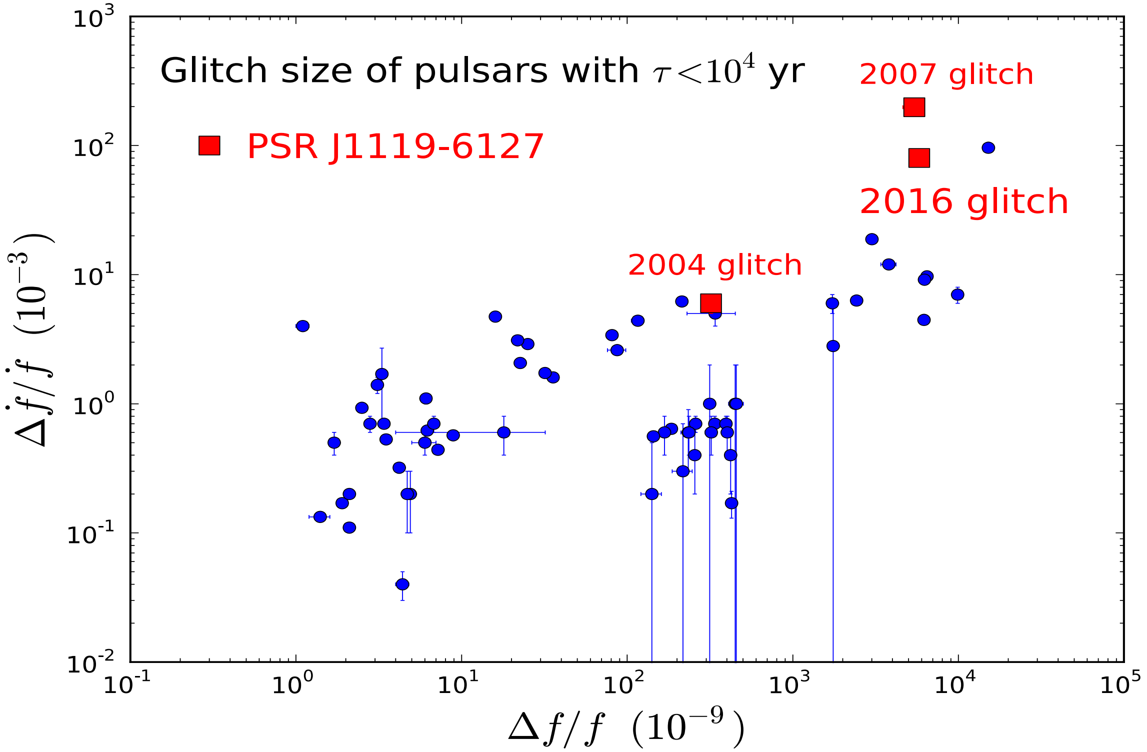

Emission during the burst

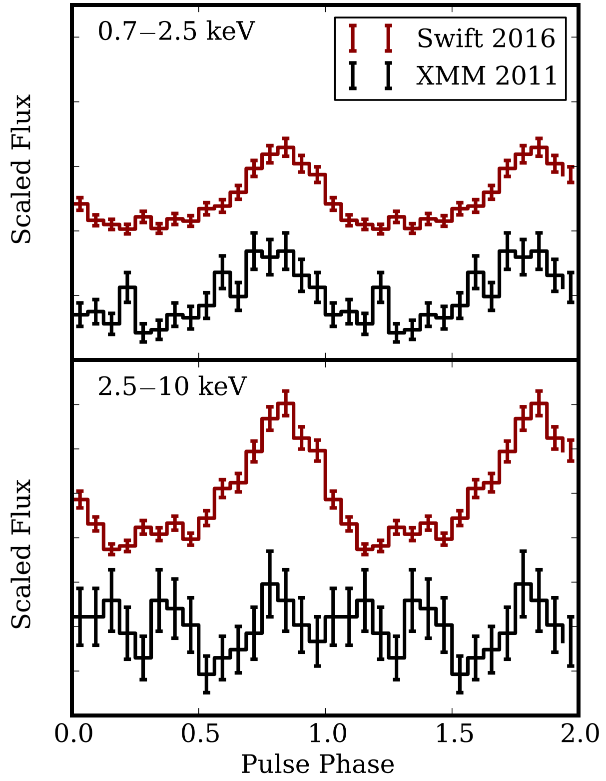

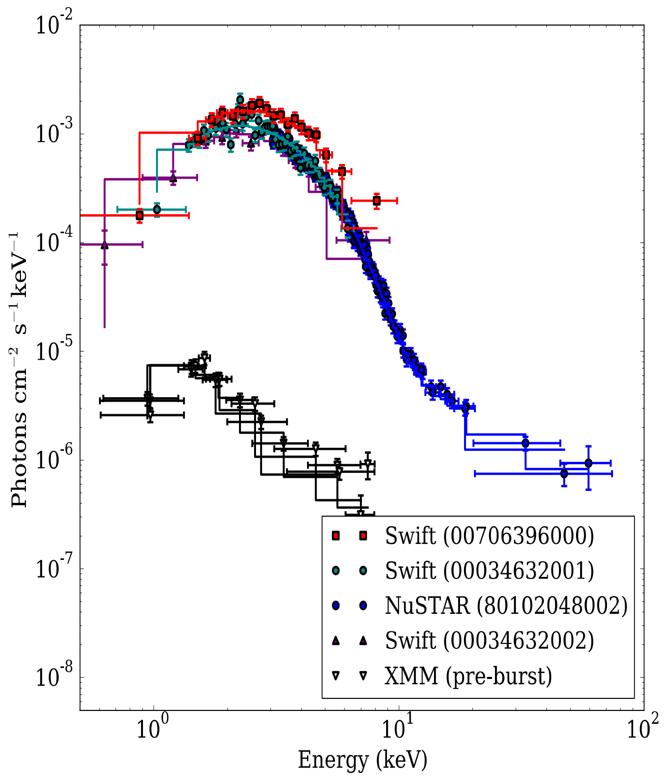

By Archibald et al.2016

- **Hard X-ray emission (>10keV) were clearly observe with a non-thermal component**
- **Surface temperature increases from ~0.2keV to ~1keV**
- **Thermal X-ray luminosity is almost 10% of the spin down power (no such other pulsars)**

Magnetically powered outburst

Motivation of this work

➢PSR J1119-6127 is the first gamma-ray pulsar that shows both rotation powered and magnetic powered activities:

◆Timing evolution after the outburst?

◆How X-ray emission evolves after the outburst?

◆How X-ray outburst affects the gamma-ray emissions?

Swift/XMM-Newton/Nustar data

X-RAY

Data events

TABLE 1

SPIN PERIODS OF PSR J11119-6127 DETEMINED BY THE X-RAY DATA AFTER 2016 OUTBURST IN THE END JULY.

Start obs. time	Instruments	Duration (ks)	ObsID	Photons	Epoch zero (MJD)	Spin frequency (Hz)	Z_1^2/H	chance prob.
2016-07-28	*Swift*/XRT	$\sim$ 35.4	00034632001	3846	57598	2.439842(1)	503/571	$< 10^{-11}$
2016-07-28	*NuSTAR*/FPM	$\sim$ 82.9	80102048002	32265	57598.5	2.4398409(2)	5820/6980	$< 10^{-11}$
2016-07-31	*Swift*/XRT	$\sim$ 17.9	00034632002	424	57600.2	2.43983(2)	28.6/47.6	5.4×10^{-7}
2016-08-05	*NuSTAR*/FPM	$\sim$ 127.0	80102048004	40275	57606.0	2.4398219(1)	7670/9310	$< 10^{-11}$
2016-08-06	*XMM*/pn	$\sim$20.1	0741732601	25530	57606.6	2.4398214(8)	7070/7990	$< 10^{-11}$
2016-08-09	*Swift*/XRT	$\sim$57.6	00034632007	1376	57606.6	2.439814(2)	151/177	$< 10^{-11}$
2016-08-09	*Swift*/XRT	$\sim$5.9	00034632008	339	57610.25	2.43979(3)	64.5/79.9	$< 10^{-11}$
2016-08-14	*NuSTAR*/FPM	$\sim$170.8	80102048006	32473	57615.0	2.4397973(1)	5340/6320	$< 10^{-11}$
2016-08-15	*XMM*/pn	$\sim$27.9	0741732701	26060	57616.0	2.4397945(6)	7020/7850	$< 10^{-11}$
2016-08-26	*Swift*/XRT	$\sim$70.5	00034632010	627	57627.0	2.439746(3)	49.4/54.1	4.0×10^{-8}
2016-08-30	*XMM*/pn	$\sim$32.5	0741732801	19904	57630.3	2.4397218(6)	4960/5540	$< 10^{-11}$
2016-08-30	*Swift*/XRT	$\sim$17.9	00034632011	542	57630.4	2.439720(8)	78.1/105	$< 10^{-11}$
2016-08-30	*NuSTAR*/FPM	$\sim$166.5	80102048008	20878	57631.0	2.4397154(2)	1810/1880	$< 10^{-11}$
2016-09-27	*Swift*/XRT	$\sim$6.4	00034632020	527	57658.05	2.43964(2)	72.7/99.9	$< 10^{-11}$
2016-12-12	*NuSTAR*/FPM	$\sim$183.3	80102048010	2118	57735.0	2.4391775(8)	175/203	$< 10^{-11}$
2016-12-13	*XMM*/pn	$\sim$47.5	0762032801	4053	57735.5	2.439177(1)	954/1020	$< 10^{-11}$

Timing evolution

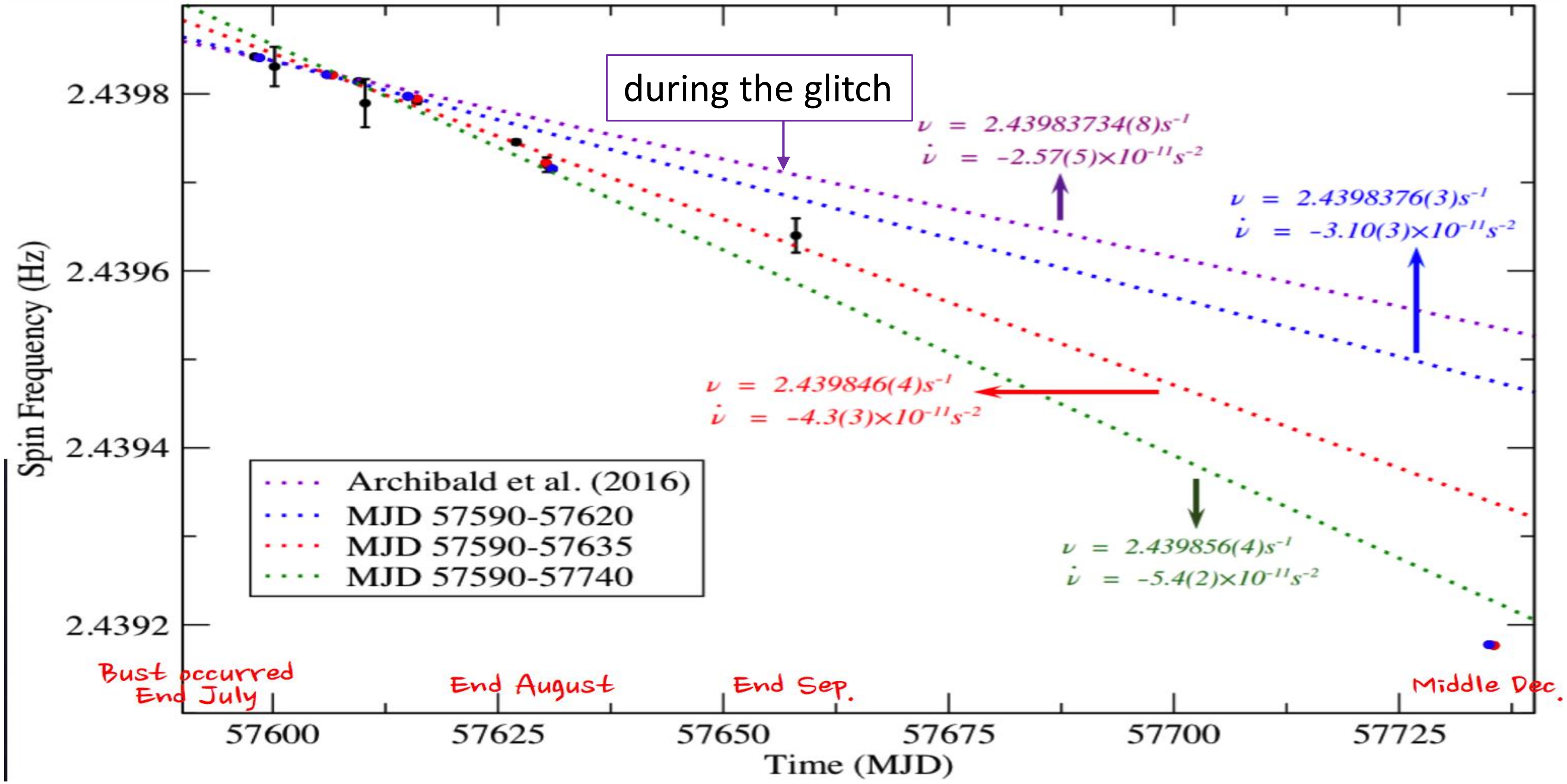

- It is naturally expected that the spin down rate gradually decreases with time after the glitch.

Spin down rate become larger with time

Radio

x-ray

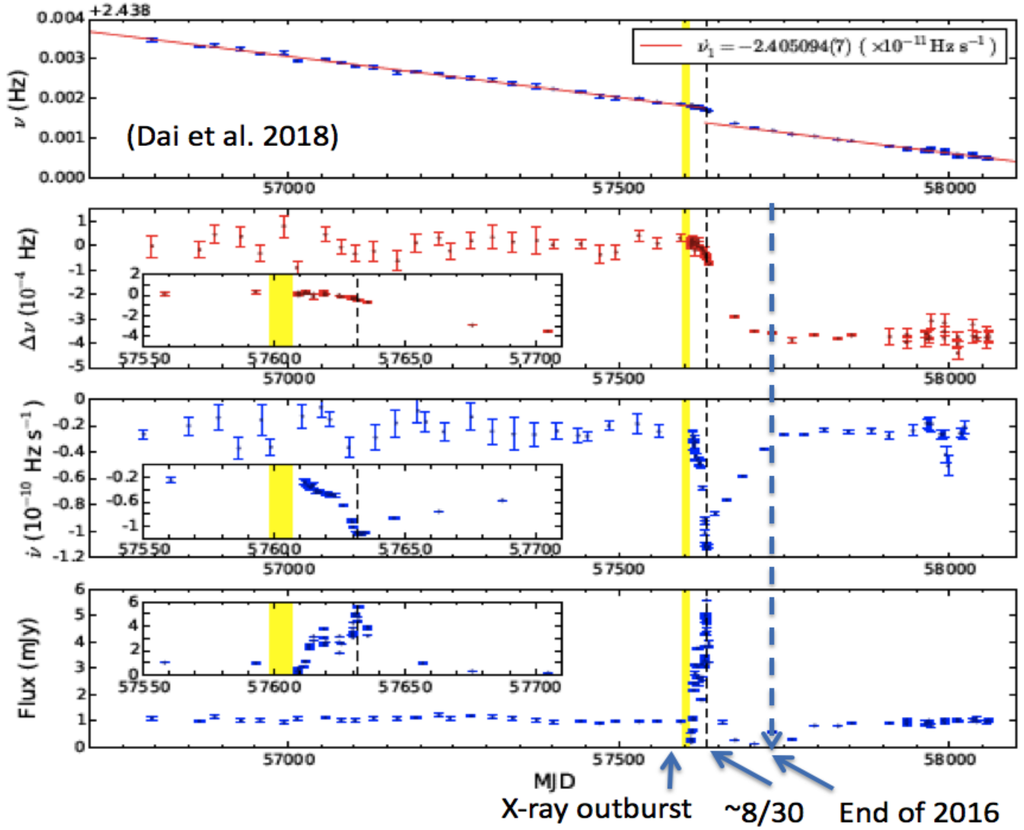

Dai.et al(2018)

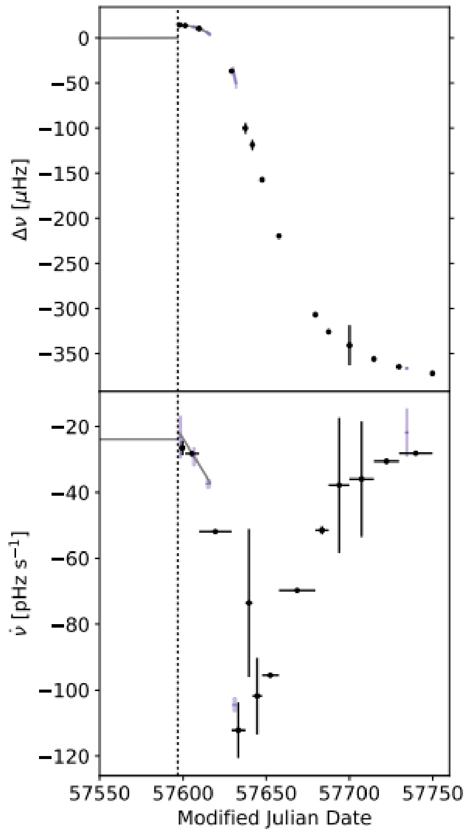

Archibald.et al(2018)

Joint xmm-newton &nustar spectrum

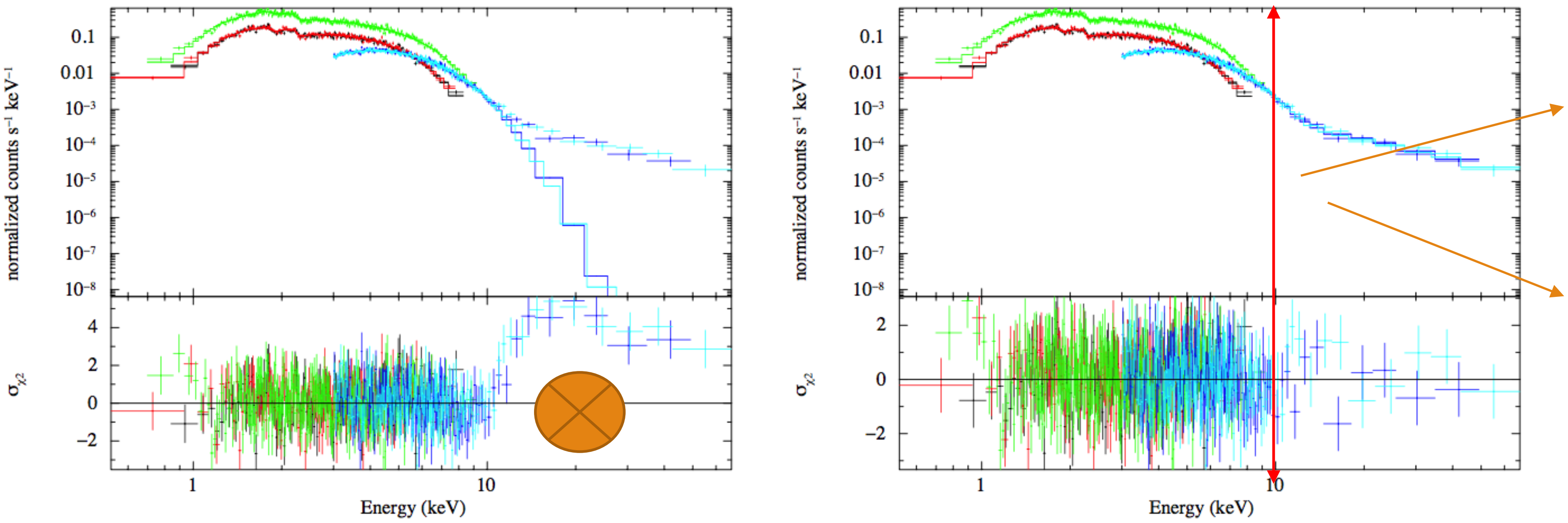

Non-thermal emission (powerlaw component)

The left panel displays the fit to the composite model of **double blackbody (2BB) components**.
The right panel presents the fit to the same model with an additional power-law component (2BB+PL)

Observed Time		Aug.05/06	Aug.14/15	Aug.30/31	Dec.12/13
	$^{a)}N_H$	$1.58^{+0.13}_{-0.12}$	$1.48^{+0.12}_{-0.11}$	$1.28^{+0.13}_{-0.11}$	$1.40^{+0.25}_{-0.22}$
	Γ	$0.56^{+0.23}_{-0.22}$	$0.21^{+0.27}_{-0.25}$	$0.41^{+0.23}_{-0.22}$	$0.62^{+2.02}_{-1.83}$
PO	$^{b)}F_{PO}$	0.023	0.010	0.020	0.002
+	kT_1 (keV)	0.32 ± 0.02	$0.33^{+0.03}_{-0.02}$	$0.36^{+0.04}_{-0.03}$	$0.35^{+0.05}_{-0.04}$
BB_1	R_1 (km)	$5.42^{+1.48}_{-1.22}$	$4.23^{+1.11}_{-0.92}$	$2.70^{+0.93}_{-0.72}$	$1.61^{+0.81}_{-0.52}$
+	$^{b)}F_{BB_1}$	0.42	0.30	0.17	0.054
BB_2	kT_2 (keV)	1.02 ± 0.01	1.04 ± 0.01	1.04 ± 0.01	$1.13^{+0.04}_{-0.05}$
	R_2 (km)	0.97 ± 0.02	$0.81^{+0.02}_{-0.01}$	$0.68^{+0.03}_{-0.02}$	0.20 ± 0.02
	$^{b)}F_{BB_2}$	1.51	1.16	0.82	0.096
	χ^2_ν/d.o.f.	1.10/954	1.05/827	1.08/828	1.01/325

Best-fit parameters of SGR/AXP observations using the CBB+PL model with *Suzaku* and *NuSTAR*.

	ObsID Month	F_{1-10}	F_{15-60}	Unabsorbed F_s,F_h SXC	HXC	N_H (10^{22} cm^{-2})	kT (keV)	R (km)	Γ_s	Γ_h	χ^2_ν (dof)
				Suzaku observations							
[illegible]	…092010	$12.6^{+0.1}_{-0.1}$	33.7(4.4)	$6.3^{+0.9}_{-0.8}$	$58.4^{+1.4}_{-1.4}$	6.7(3)	0.61(4)	1.8	···	1.62(5)	0.97 (377)
1806−20	401021010	$10.5^{+0.1}_{-0.2}$	21.1(3.3)	$3.4^{+0.9}_{-0.8}$	$50.1^{+2.9}_{-2.6}$	5.5(5)	0.68(9)	1.1	···	1.51(9)	1.18 (171)
1806−20	402094010	$8.9^{+0.1}_{-0.2}$	27.1(4.3)	$5.9^{+1.0}_{-0.8}$	$42.2^{+1.8}_{-1.7}$	6.5(5)	0.65(6)	1.5	···	1.50(7)	1.22 (193)
1841−04	401100010	$19.4^{+0.1}_{-0.1}$	48.9(0.3)	$35.1^{+1.4}_{-1.4}$	$50.9^{+2.2}_{-2.1}$	2.5(1)	0.27(1)	21.1	3.41(10)	0.87(8)	1.22 (2087)
1900+14	401022010	$5.3^{+0.5}_{-0.5}$	20.6(5.5)	$4.6^{+0.1}_{-0.6}$	$25.0^{+3.2}_{-3.4}$	1.8(3)	0.57(2)	2.5	···	0.96(14)	1.13 (44)
1900+14	404077010	$4.3^{+0.1}_{-0.1}$	16.5(3.5)	$4.5^{+0.3}_{-0.3}$	$26.3^{+2.9}_{-2.5}$	1.9(1)	0.52(2)	3.0	···	0.78(9)	1.34 (57)
1714−38	501007010	$1.7^{+0.1}_{-0.1}$	···	$5.0^{+0.5}_{-0.3}$	···	3.5(1)	0.24(4)	15.7	3.25(8)	···	1.28 (179)
1708−40	404080010	$38.1^{+0.5}_{-0.2}$	24.4(4.4)	$69.1^{+3.5}_{-3.3}$	$28.4^{+2.8}_{-2.7}$	1.3(1)	0.26(2)	14.2	3.48(9)	0.67(24)	0.98 (394)
1708−40	405076010	$35.8^{+0.4}_{-0.1}$	24.4(4.0)	$55.0^{+4.0}_{-2.7}$	$33.4^{+2.1}_{-2.2}$	1.2(1)	0.30(1)	9.5	3.80(21)	1.14(16)	1.05 (540)
1048−59	403005010	$9.9^{+0.1}_{-0.1}$	< 13.2	$12.3^{+0.2}_{-0.2}$	< 19.5	0.47(3)	0.45(1)	4.7	4.88(20)	···	1.32 (78)
0142+61	402013010	$122.0^{+0.1}_{-0.1}$	35.1(6.4)	$185.1^{+0.7}_{-0.7}$	$38.3^{+2.3}_{-2.3}$	0.61(1)	0.28(1)	19.0	4.68(2)	0.24(7)	1.43 (1725)
0142+61	404079010	$115.6^{+0.2}_{-0.2}$	26.2(5.8)	$176.8^{+1.5}_{-1.5}$	$27.1^{+2.3}_{-2.2}$	0.62(1)	0.28(1)	18.6	4.71(4)	0.39(14)	1.15 (1401)
0142+61	406031010	$108.3^{+1.1}_{-0.9}$	24.3(3.7)	$164.8^{+4.6}_{-4.4}$	$41.3^{+4.1}_{-4.0}$	0.63(3)	0.28(1)	18.0	4.65(10)	0.32(21)	1.08 (1062)
0142+61	408011010	$107.8^{+0.4}_{-0.4}$	19.1(2.8)	$162.7^{+1.4}_{-1.4}$	$32.9^{+2.3}_{-2.2}$	0.60(1)	0.28(1)	17.9	4.81(4)	0.26(11)	1.37 (838)
2259+58	404076010	$30.4^{+0.1}_{-0.1}$	< 10.1	$44.8^{+0.5}_{-0.5}$	< 14.9	0.55(1)	0.29(1)	7.8	4.85(4)	[illegible]	1.20 (510)
1818−15	406074010	$1.0^{+0.1}_{-0.1}$	···	$1.4^{+0.1}_{-0.1}$	···	2.1(21)	1.61(6)	0.1	···	···	1.31 (83)
1547−54	903006010	$59.7^{+0.9}_{-0.8}$	110.2(5.2)	$50.6^{+1.7}_{-1.7}$	$158.7^{+3.3}_{-3.3}$	2.8(1)	0.67(2)	1.9	···	1.53(4)	1.29 (140)
1547−54	405024010	$11.1^{+0.1}_{-0.2}$	13.5(3.3)	$17.5^{+0.6}_{-0.6}$	$23.4^{+2.5}_{-2.4}$	2.8(1)	0.62(1)	1.3	···	1.15(12)	1.23 (69)
0501+45	903002010	$36.2^{+0.3}_{-0.2}$	28.1(6.5)	$42.2^{+0.6}_{-0.8}$	$30.4^{+4.0}_{-3.7}$	0.40(2)	0.49(1)	2.7	4.35(17)	0.10(35)	1.23 (206)
0501+45	404078010	$2.9^{+0.1}_{-0.1}$	< 20.9	$3.8^{+0.3}_{-0.2}$	< 30.8	0.44(10)	0.30(3)	2.2	4.16(27)	···	0.92 (77)
0501+45	405075010	$1.7^{+0.1}_{-0.1}$	< 16.2	$2.0^{+0.2}_{-0.2}$	< 23.9	0.24(13)	0.30(4)	1.6	4.20(45)	···	0.80 (34)
0501+45	408013010	$1.7^{+0.1}_{-0.1}$	< 12.7	$2.3^{+0.1}_{-0.1}$	< 18.8	0.41(7)	0.26(2)	2.3	3.79(15)	···	0.96 (367)
1833−08	904006010	$3.8^{+0.1}_{-0.1}$	17.6(4.5)	$7.9^{+0.3}_{-0.2}$	$35.6^{+9.3}_{-8.8}$	9.6(5)	1.08(4)	0.7	···	−0.38(40)	1.37 (167)
1647−45	901002010	$27.2^{+0.1}_{-0.1}$	···	$45.9^{+0.5}_{-0.5}$	···	1.7(1)	0.49(1)	3.4	4.39(6)	···	1.26 (248)
1822−16	906002010	$18.2^{+0.4}_{-0.3}$	< 4.9	$18.5^{+0.5}_{-0.4}$	< 7.2	0.02(4)	0.54(2)	0.7	5.86(71)	···	1.41 (59)

- **The emission with a very hard non-thermal component is also similar to the magnetar's emission**

Magnetar-like emission after the burst

evolution

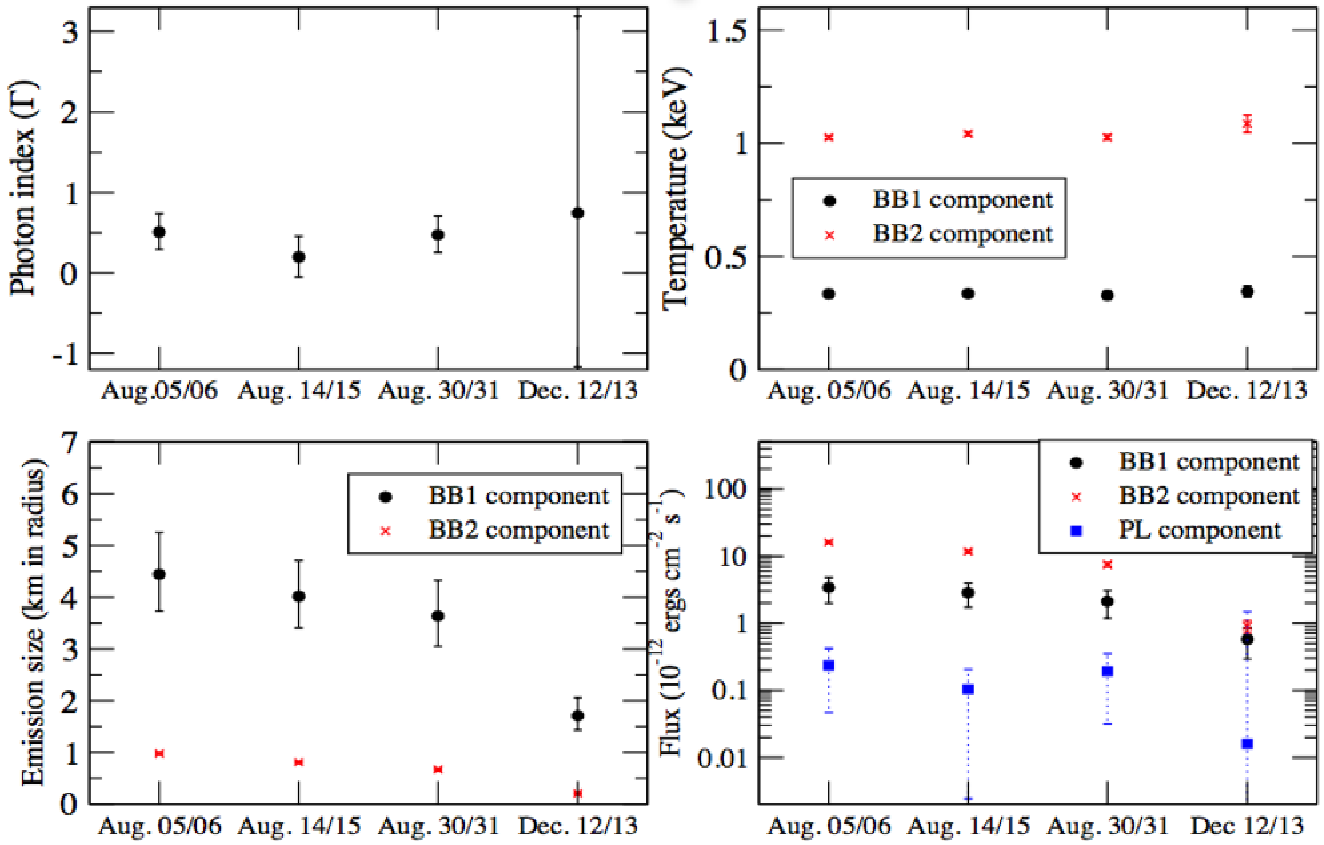

- ➢ The X-ray flux continuously decreased with time
- →Surface temperature was almost constant (at least until 6 months after the burst)
- →The emission size decreased.

- ➢ No significant no-thermal component was observed after December.

larger hotspot replaced by the magnetized atmospheric radiation

	Observed Time	Aug.05/06	Aug.14/15	Aug.30/31	Dec.12/13
	a) N_H	$1.58^{+0.13}_{-0.12}$	$1.48^{+0.12}_{-0.11}$	$1.28^{+0.13}_{-0.11}$	$1.40^{+0.25}_{-0.22}$
	Γ	$0.56^{+0.23}_{-0.22}$	$0.21^{+0.27}_{-0.25}$	$0.41^{+0.23}_{-0.22}$	$0.62^{+2.02}_{-1.83}$
PO	b) $F_{\rm PO}$	0.023	0.010	0.020	0.002
+	kT_1 (keV)	0.32 ± 0.02	$0.33^{+0.03}$ [illegible]	$0.36^{+0.04}$ [illegible]	$0.35^{+0.05}$ [illegible]
BB_1	R_1 (km)	$5.42^{+1.48}_{-1.22}$	$4.23^{+1.11}_{-0.92}$	$2.70^{+0.93}_{-0.72}$	$1.61^{+0.81}_{-0.52}$
+	b) $F_{\rm BB_1}$	0.42	0.30	0.17	0.054
BB_2	kT_2 (keV)	1.02 ± 0.01	1.04 ± 0.01	1.04 ± 0.01	$1.13^{+0.04}_{-0.05}$
	R_2 (km)	0.97 ± 0.02	$0.81^{+0.02}_{-0.01}$	$0.68^{+0.03}_{-0.02}$	0.20 ± 0.02
	b) $F_{\rm BB_2}$	1.51	1.16	0.82	0.096
	χ^2_ν/d.o.f.	1.10/954	1.05/827	1.08/828	1.01/325

	a) N_H	$1.50^{+0.06}_{-0.05}$	$1.50^{+0.06}_{-0.04}$	1.47 ± 0.06	$1.83^{+0.13}_{-0.12}$
PL	Γ	$0.50^{+0.23}_{-0.21}$	$0.18^{+0.26}_{-0.25}$	0.44 ± 0.22	$-0.17^{+0.96}_{-1.58}$
+	b) $F_{\rm PL}$	0.021	0.010	0.021	0.002
c) nsa	kT_1 (eV)	230 ± 6	222^{+6}_{-5}	211 ± 5	175^{+4}_{-5}
+	b) $F_{\rm nsa}$	0.40	0.35	0.28	0.12
BB	kT_2 (keV)	1.03 ± 0.01	1.04 ± 0.01	1.03 ± 0.01	$1.10^{+0.04}_{-0.03}$
	R (km)	$0.95^{+0.01}_{-0.02}$	$0.80^{+0.02}_{-0.01}$	$0.70^{+0.01}_{-0.02}$	$0.21^{+0.02}_{-0.01}$
	b) $F_{\rm BB}$	1.48	1.15	0.83	0.10
	χ^2_ν/d.o.f.	1.11/955	1.05/828	1.08/829	1.00/282
	a) N_H	$1.53^{+0.04}_{-0.05}$	1.54 ± 0.05	1.51 ± 0.06	$1.88^{+0.11}_{-0.12}$
PL	Γ	0.49 ± 0.22	0.16 ± 0.25	$0.42^{+0.23}_{-0.22}$	$-0.52^{+1.20}_{-1.41}$
+	b) $F_{\rm PL}$	0.021	0.0096	0.020	0.001
d) nsmax	kT_1 (eV)	245 ± 6	238 ± 5	225 ± 6	187 ± 5
+	b) $F_{\rm nsmax}$	0.45	0.40	0.32	0.14
BB	kT_2 (keV)	1.03 ± 0.01	1.05 ± 0.01	1.04 ± 0.01	1.12 ± 0.04
	R_2 (km)	$0.94^{+0.01}_{-0.02}$	$0.80^{+0.01}_{-0.02}$	$0.69^{+0.01}_{-0.02}$	$0.21^{+0.01}_{-0.02}$
	b) $F_{\rm BB_2}$	1.47	1.14	0.82	0.099
	χ^2_ν/d.o.f.	1.12/955	1.06/828	1.08/829	1.00/282

Fermi data

GAMMA-RAY

Gamma ray : Fermi(LAT)

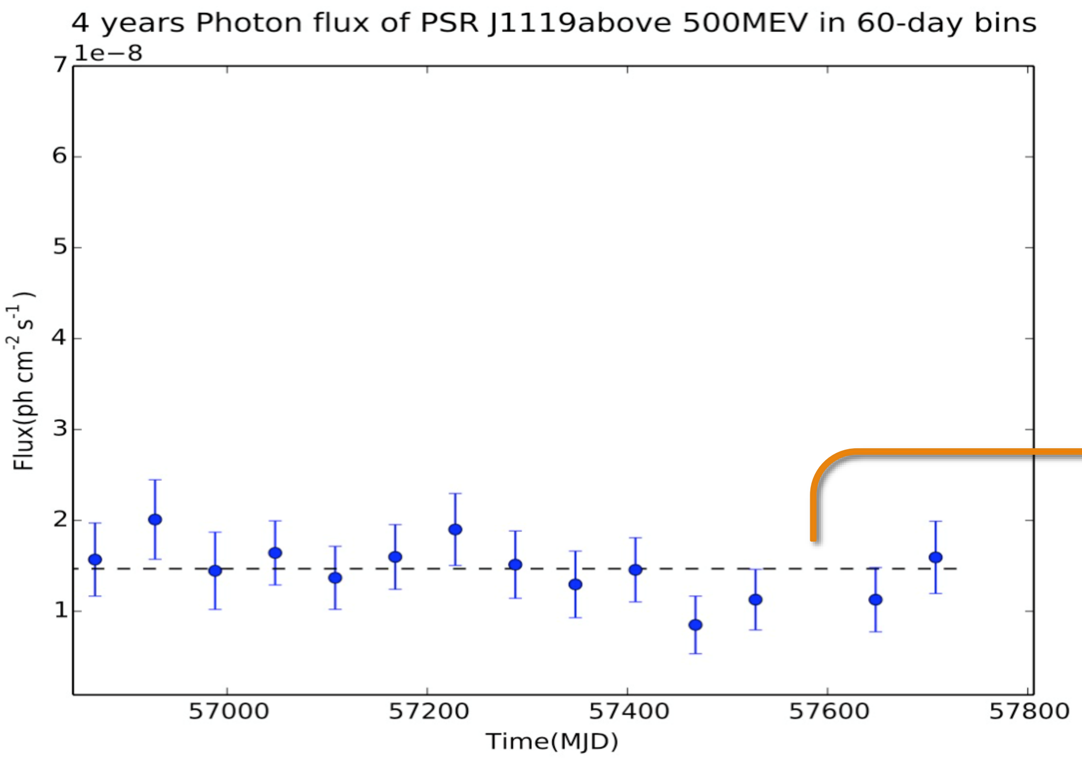

MJD 56900-57560 (660 days before the outburst):

$F_{0.5\text{-}100GeV}$ = (1.20±0.10)x10^(-11) ergs cm^{-2} s^{-1}

MJD 57566-57630 (64 days during and after the outburst):

$F_{0.5\text{-}100GeV}$ = 4.9x10^(-12) ergs cm^{-2} s^{-1}

MJD57596=2016/07/27

The time of burst and glith

- As significant drop of photon flux was observed.

Gamma-ray model

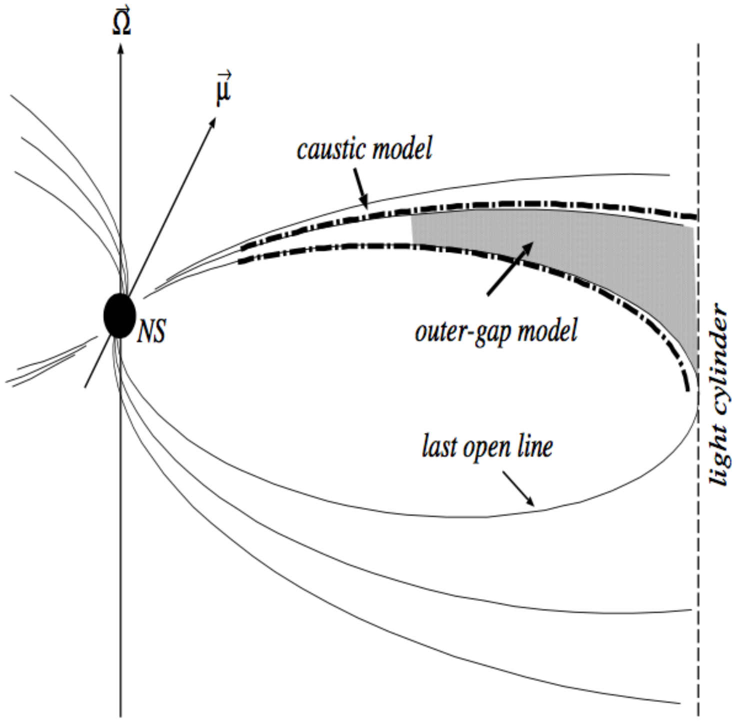

k.S cheng 1986

- The drop of GeV flux can be explained by the change of the emission size at the outburst.
- GeV gamma-rays from the outer gap (Cheng et al. 1986)
- The radiation power of the gap is on the order of :

$$L_\gamma \sim f_{gap} I_{GJ} \times f_{gap}^2 \Phi_a \sim f_{gap}^3 L_{sd} .$$

$$f_{gap} \equiv \frac{\delta\theta}{\theta_{pc}} .$$

where fgap represents a fraction of the open magnetic field lines that penetrate the outer gap.

Gamma-ray theory

gamma-ray emission by curvature radiation

$$E_\gamma = \frac{3}{4\pi}\frac{hc\Gamma_c^3}{R_c} \sim 1\mathrm{GeV}\left(\frac{f_{gap}}{0.3}\right)^{3/2}\left(\frac{B_s}{10^{12}\,\mathrm{G}}\right)^{3/4}\left(\frac{\Omega}{100\,\mathrm{s}^{-1}}\right)^{5/4}\left(\frac{r}{\varpi_{lc}}\right)^{-1/8}.$$

- The gap fraction is determined by the condition of the photon-photon pair creation process

$$E_X E_\gamma(1 - \cos\theta_{X\gamma}) \geq 2(m_e c^2)^2$$

Where the energy of x-ray can be get from the observed data ,

- the flux is proportional to fgap, $L_\gamma \sim f_{gap} I_{GJ} \times f_{gap}^2 \Phi_a \sim f_{gap}^3 L_{sd}$.

Gamma ray flux

states	Ex(kev)	Egamma(gev)	fgap	Lgamma(erg/s)
before	0.2	1.5	0.393	1.4×10^{35}
after	1.0	0.2	0.1	2×10^{33}

- We expect that gamma-ray flux after the outburst about two order of magnitude smaller than that before the outburst.
- At ~6 months after the outburst, the thermal emission is quickly decreasing, which causes the recovery of the GeV emission.

conclusion

- Different from other magnetars and high-B pulsars or the previous two glitches occurred in 2004 and 2007 of PSR J1119, there was a large glitch at X-ray outburst, and then caused a drastic spin-down until August 30,and recovery finished until the end of 2016.
- The X-ray pulsations can be described by the contribution from two hotspots (less than 10kev) , and the surface emission from the larger hotspot can be replaced by the magnetized atmospheric radiation.
- We discussed the gamma-ray dropped photon flux by the theoretical model

Thank you for listening

Fermi/GBM light curves of the 2016 July 27 PSR J1119−612 burst in three energy ranges (Göğüş et al., 2016).

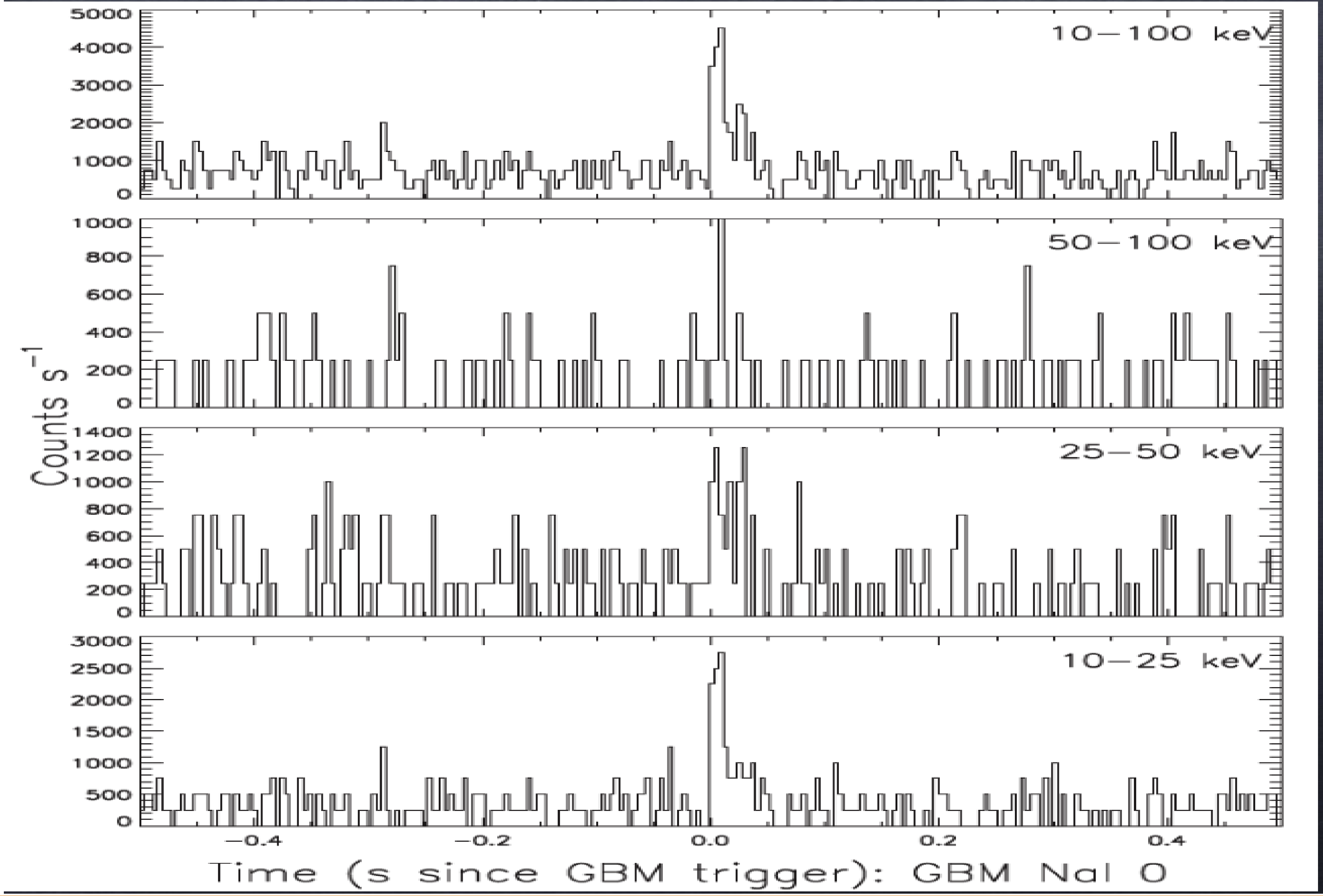

Magnetars

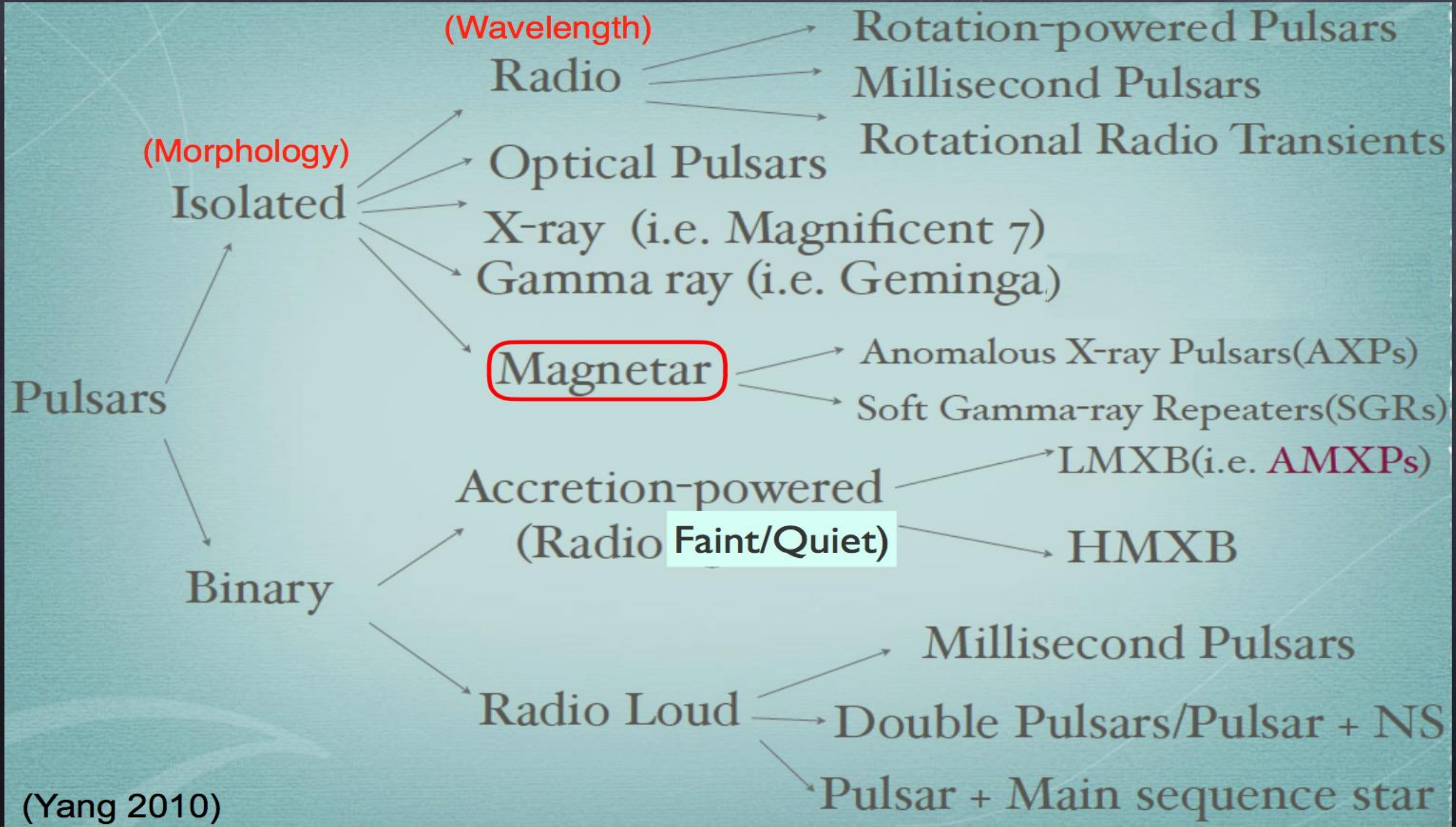
(Wavelength)
Radio
Rotation-powered Pulsars
Millisecond Pulsars
Rotational Radio Transients
(Morphology)
Isolated
Optical Pulsars
X-ray (i.e. Magnificent 7)
Gamma ray (i.e. Geminga)
Magnetar
Anomalous X-ray Pulsars(AXPs)
Soft Gamma-ray Repeaters(SGRs)
Pulsars
LMXB(i.e. AMXPs)
Accretion-powered
(Radio Faint/Quiet)
HMXB
Binary
Millisecond Pulsars
Radio Loud
Double Pulsars/Pulsar + NS
Pulsar + Main sequence star
(Yang 2010)

Quick Summary

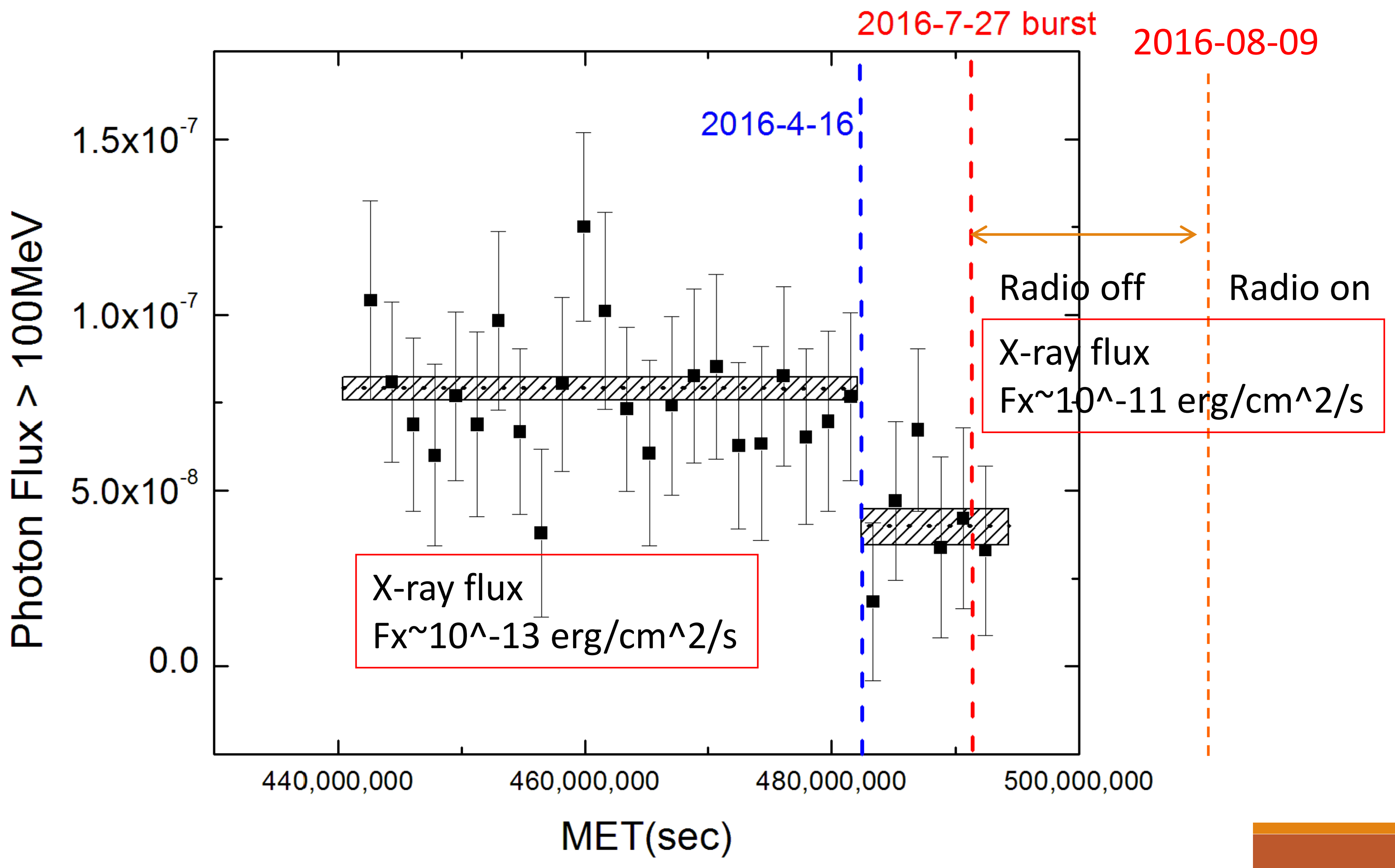

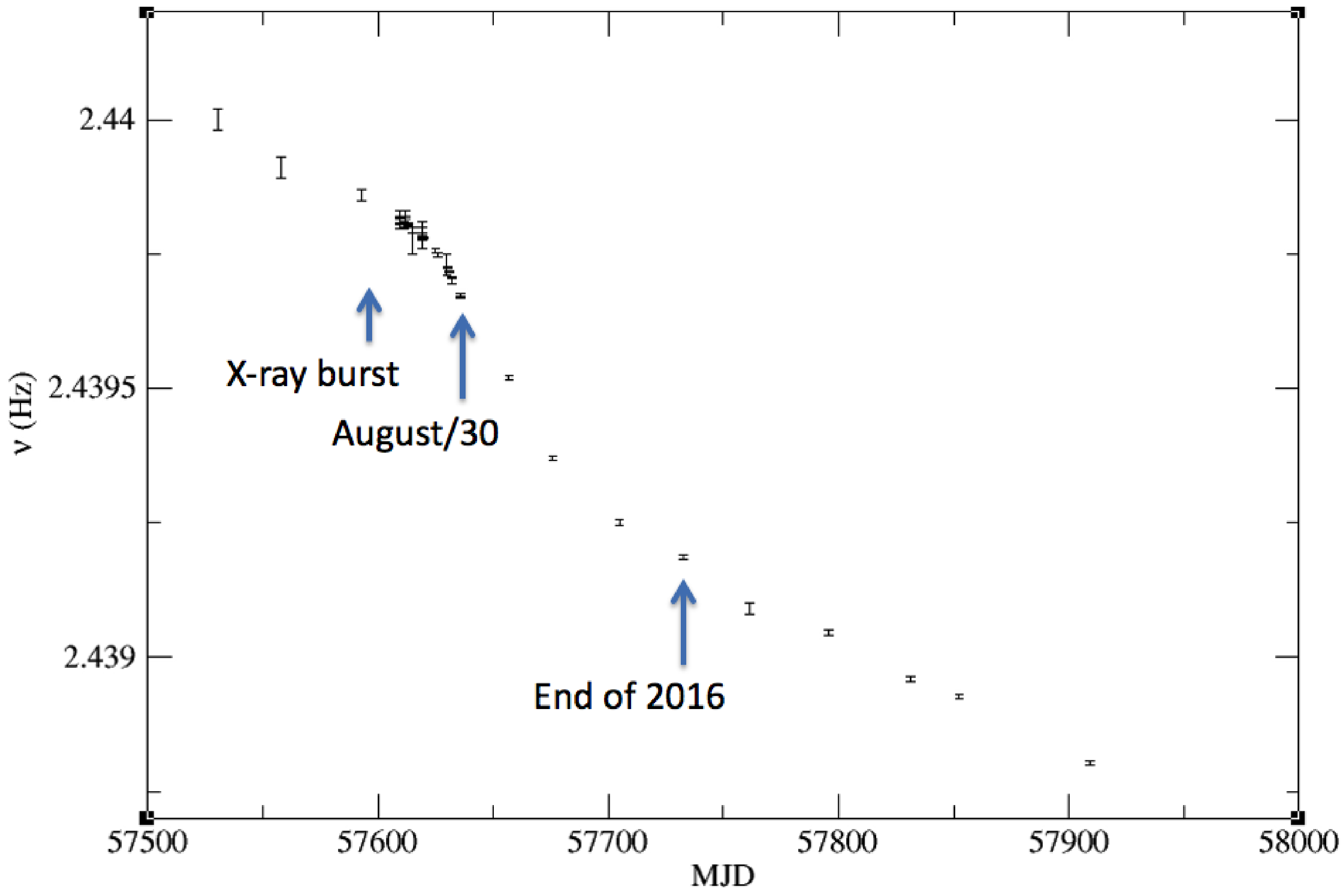

2.44
2.4395
2.439
ν (Hz)
57500
57600
57700
57800
57900
58000
MJD
X-ray burst
August/30
End of 2016

e a spin-up glitch with $\Delta\nu = 1.40(2) \times 10^{-5}$ Hz

$$\Delta\dot{\nu} = -1.9(5) \times 10^{-12}\,\text{Hz s}^{-1}.$$

1. Introduction

- Glitch Mechanisms

- A *sudden release of the stress* built up in (i) solid crust or (ii) pinned vortices in the superfluid interior.

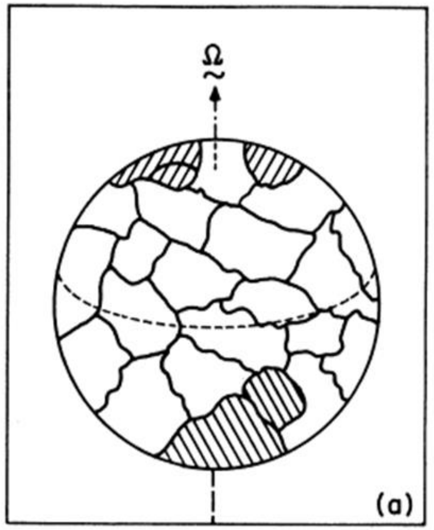

(i) Starquake model (Ruderman 1969)

- Release the stress stored in solid cru
- Rearrangement of the solid crusts.
- Small glitch.

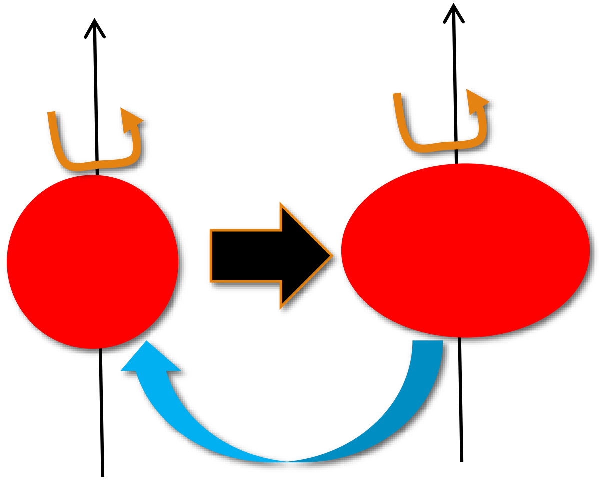

glitch

1. Introduction

- Glitch Mechanism

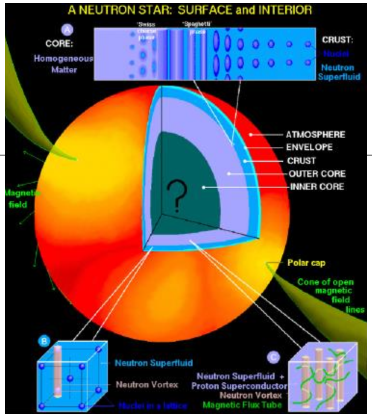

(2) Unpinned model (Alper et al. 1984)

- Proton and neutron superfluid at the core

- Formations of many vortices.

- *Magnetic field are pinned at vortices*
  (lower energy state of the system)

- Differential rotation between the crust and core produces the stress at pinned vortices.

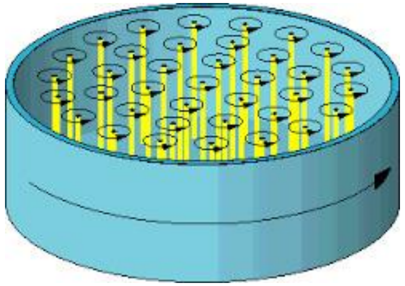

- Sudden spin up due to *unpin* (large glitch).

Evolution of the pulse profile

- the folded light curves in the soft X-ray (< 2.5 keV) and the medium X-ray (3– 10 keV) bands have no significant structure change with aligned pulsed peaks

- Single pulse profile <10keV with a marginal detection of the second peak.

- Pulse detection (marginal) >10keV just after the burst, but no detection after in Aug

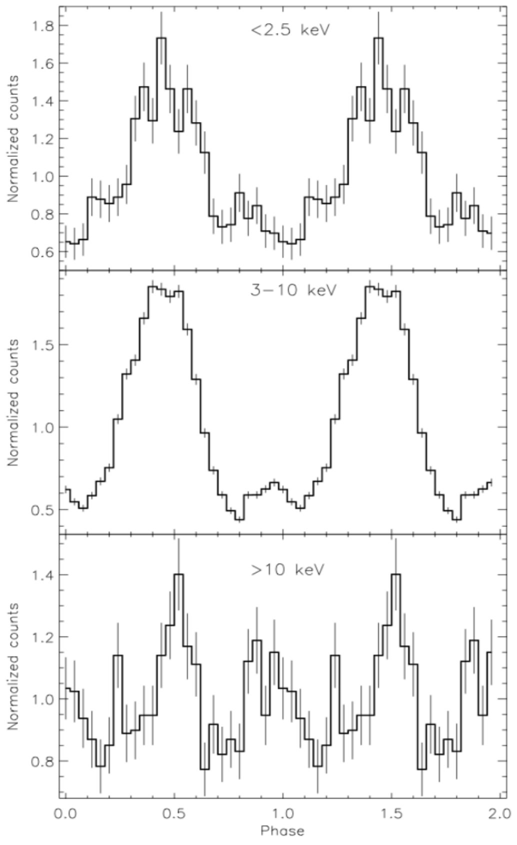

observed on July 28/29 of 2016

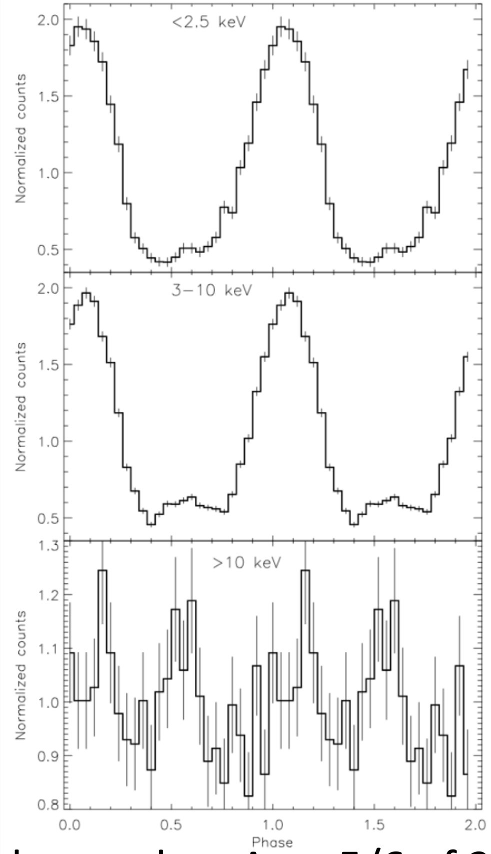

observed on Aug. 5/6 of 2016